SINERGI Vol. 22, No.2, June 2018: 83-90
DOAJ:doaj.org/toc/2460-1217
DOI:doi.org/10.22441/sinergi.2018.2.003 .

THE EFFECT OF 3D PRINTING MACHINE PARAMETERS IN EXTRUSION PROCESS OF BIOCOMPOSITE MATERIALS (PMMA AND HA) ON DIMENSIONAL ACCURACY

Raeshifa Diani Almy, Alva Edy Tontowi
Industrial Engineering Department, Faculty of Engineering, Universitas Gadjah Mada
Jl. Grafika No.2, Yogyakarta 55281
Email: raeshifa.diani.a@ugm.ac.id, alvaedytontowi@ugm.ac.id

Abstract -- *Bone implants are medical procedures involving replacement or reconstruction of missing or damaged bones with the patient's ones, natural substitutes or artificial substitutes. The widely used bone cement is a polymethylmethacrylate (PMMA) based composite material. To improve bioactivity, PMMA is combined with hydroxyapatite (HA). The manual formation can make bone implants during surgery. However, the method requires a longer operation time and raises the possibility of a higher error. Therefore, 3D printing technology is used to improve the quality of bone implants. One of the machines that can be used is the 3D printing machine, the property of the Product Design and Development Laboratory of Universitas Gadjah Mada. This machine needs to be tested to determine the accuracy of the prints, which is one indicator of product quality. Several machine parameters can be set in this machine setting. This study aims to determine the effect of three parameters, those are perimeter speed or edge print speed (20-40 mm / s), infill speed or inner print speed (50 - 70 mm / s), and fill angle or inner slope of inner printing (45 - 90 ° C). Before printing complex shapes, the machine was tested in advance with a more straightforward specimen design, which is a specimen design of flexural strength test. Response surface experiment design is used to determine the effect of three parameters on the dimensional accuracy which is measured through dimensional error. The results show that these three factors have no significant impact on the dimensional error, but the resulting error is still high. Therefore, it is necessary to adjust the design size before printing.*
.

Keywords: *3D printing; Perimeter speed; Hydroxyapatite; Polymethilmethacrilate (PMMA); Dimension error*

Received: January 26, 2018 *Revised: April 18, 2018* *Accepted: April 18, 2018*

INTRODUCTION

In the 1980s since Charles Hull published his research on stereolithography in 1986 3D printing technology has been known (Wang et al., 2016). However, 3D printing applications in the medical field began to overgrow in early 2000, especially for the manufacture of denture and dental implants (Lim et al., 2014).

Bone grafting or bone implant is surgical procedures involving replacement or reconstruction of lost or damaged bones from the patient's own body, natural substitutes or artificial substitutes (Mao, 2013 in Schickert, 2014). Bone implants have been started since the 1800s. Implant material at the time was made of human bones (Macewen, 1881 in Schickert, 2014).

At present, there are more types of bone implant materials, such as allograft, autograft, bioactive glass, bioceramics, metal-based implants, polymer/plastic implants, etc. (Puska et al, 2011). The most widely used materials as bone cement in recent years are polymethylmethacrylate or PMMA based composites (Puska et al, 2011 and Zebarjad et al, 2011). Pure PMMA has limited mechanical properties, less compatible, rigid, and non-bioactive (Zebarjad et al, 2011). To improve bioactivity, PMMA-based cement is combined with inorganic substances, such as bioactive hydroxyapatite (HA) (Puska et al, 2011).

Biocomposite mixtures can be formed into bone implants manually or by a 3D printing method. According to Saldarriaga et al (2011) in Castelan et al. (2014), the use of manufacturing technologies such as 3D printing can reduce operating time by up to 85% (Köksal et al., 2011), restore the patient's body shape precisely as before, reduce errors in the operation process, avoid modification of the implant area around injury during operation, and the printed model can be used as an effective communication tool to the patient's family. These advantages make this technology intensively developed to achieve a good quality implant (Mohammed et al., 2016; Lamboni et al., 2015; Serbetci et al., 2004).

One type of machine that can be used is a 3D printing machine owned by the Product Design and Development Laboratory of

Universitas Gadjah Mada. The shape of the machine is shown in Fig. 1. This machine still needs to be tested to determine its ability to print accurate products in accordance with the design that has been made.

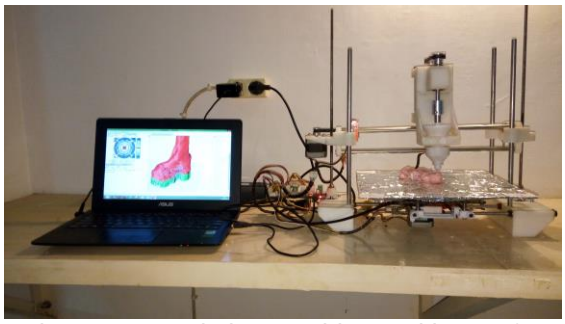

Figure 1. 3D printing machine and laptop for operation

To use this machine, the material is fed to the material container. Inside is a screw system that will push the material gradually and remove it through a nozzle measuring 1.5 mm. Before it can be used to create functional products in various forms such as implants, this machine needs to be tested first by printing a simpler form.

According to Mohamed et al (2015), there are several process parameters that can affect the quality and mechanical properties of extrusion components of 3D printing machines, namely concept models, materials, machine parameters, environmental factors, machine movement direction, and work parameters. The parameter is the input of the process, while the response of the parameter is the output of the process.

This research was conducted to know the effect of machining parameters on extrusion process of biocomposite polymer to dimension error of bending test specimen. Input process to be observed is Perimeter Speed, Infill Speed, and Fill Angle. The machining parameters can be set with the Printrun Pronterface software, which is open source 3D printing software and licensed under the GNU General Public License. The observed process output is the accuracy of the flexural strength test specimen dimension, which includes dimensions of length, width, and height. This specimen was chosen because of its simple shape. The materials used are PMMA heat curing and hydroxyapatite as in Tontowi et al. (2017). In this study hydroxyapatite is used up to 25% of PMMA powder, but in this study the composition of hydroxyapatite will be increased up to 50% of PMMA powder. This study aims to observe whether differences in machine settings affect the error between the design dimensions of specimens with the dimensions of printing.

MATERIALS AND METHOD

Prior to printing, the specimen is designed first with Autodesk Inventor software. The specimen design used was ASTM D 790 specimens. The recommended specimen size was 127mm x 12.7 mm x 3.2mm. However, in this study the length and width of the specimen was slightly enlarged due to fear of shrinkage at the time the specimens dried up. The shape and size of the specimen are shown in Fig. 2.

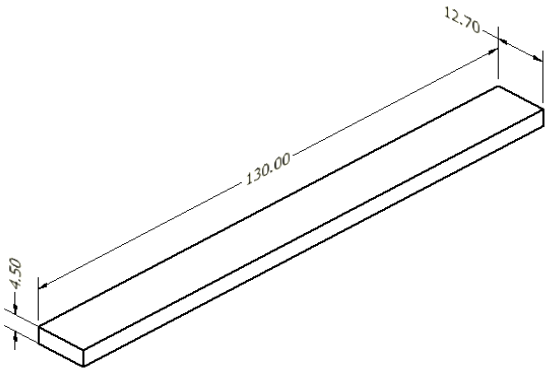

Figure 2. Design specimen ASTM D790 with modification (in mm)

The specimen design is then converted into * .stl format and then inserted into Slic3r, the slicing software that is part of the Printrun Pronterface software. In Slic3r software, there are several adjustable machine parameters as shown in Fig. 3.

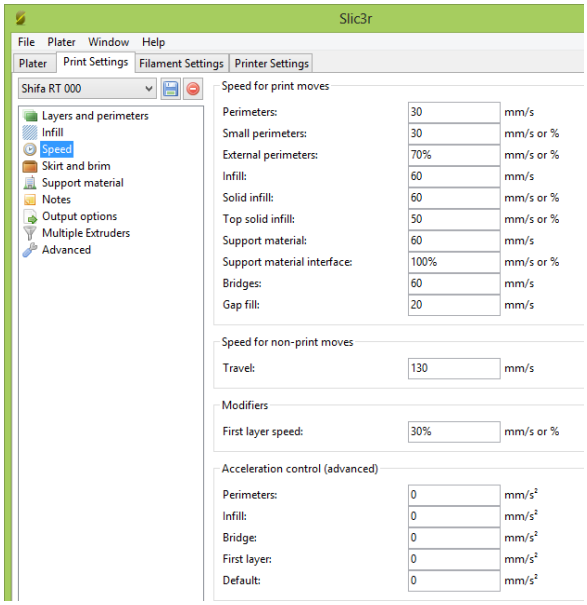

Figure 3. Setting of machine parameters with Sic3r

From preliminary observations by running the machine, the value of the machine parameters is obtained and shown in Table 1. Using the response surface reaction design, there are 20 parameter settings as shown in Table 2. The response surface method is selected because it can test the relationship between response variables and a set of experimental variables with some variable levels (Bezerra et al, 2008). This method has also been widely used in research in manufacturing (Koksal et al, 2011)

Table 1. Machine Parameter

Independent Variable	Parameter
Perimeter speed (mm/s)	20 – 40
Infill Speed (mm/s)	50 – 70
Fill Angle (°)	45 – 90

Twenty settings on the experimental design will be incorporated into the Slic3r software that translates the * .stl format into a * .gcode format. The program is then inserted and read by the Printrun Pronterface as shown in Fig. 4.

Table 2. Experiment Design

Run Order	Machine Parameter			Coded Variable		
	Peri-meter Speed	Infill Speed	Fill Angle	A	B	C
1	30	60	67,5	0	0	0
2	20	50	90	-1	-1	1
3	30	60	67,5	0	0	0
4	20	70	45	-1	1	-1
5	20	50	45	-1	-1	-1
6	30	60	67,5	0	0	0
7	40	70	90	1	1	1
8	40	50	90	1	-1	1
9	40	70	45	1	1	-1
10	30	60	67,5	0	0	0
11	20	70	90	-1	1	1
12	40	50	45	1	-1	-1
13	30	60	30,76	0	0	-1,63
14	13,67	60	67,5	-1,63	0	0
15	46,33	60	67,5	1,63	0	0
16	30	60	67,5	0	0	0
17	30	60	67,5	0	0	0
18	30	60	104,24	0	0	1,63
19	30	43,67	67,5	0	-1,63	0
20	30	76,33	67,5	0	1,63	0

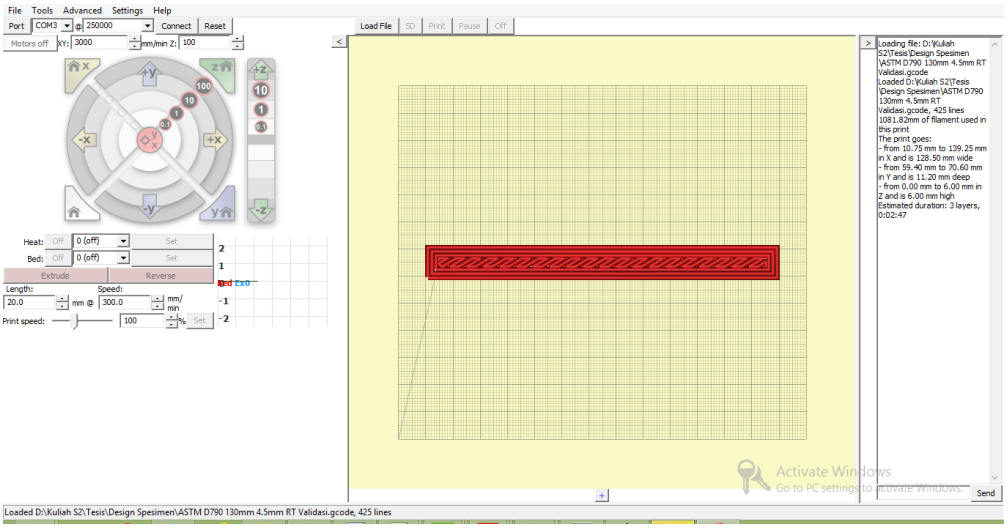

Figure 4. Main display of Printrun Pronterface

The material used in this research is a set of polymethylmethacrylate (PMMA) powder and methylmethacrylate (MMA) liquid of Acrylic Denture Materials brand and Bionanocarbonate brand hydroxyapatite Hydroxyapatite BATAN. The composition used in this study is the ratio of mass and volume of PMMA : MMA = 1 : 1 with hydroxyapatite by 20% of the total mixture. The material composition used in this study was obtained after experimenting with several material compositions in the laboratory to find a mixture that can flow through a 1.5 mm nozzle has the best compression strength.

The powdered material is mixed first until uniform for 1 minute. After that, the liquid material (MMA) is inserted and mixed evenly for 1 minute. The machine is then turned on and connected to a computer with the Printrun Pronterface software. The biocomposite mixture is then fed into the funnel and extruded at a speed of 60 mm / min and 80 mm / min. The mixture continues to be extruded to produce a continuous flow as shown in Fig. 5. To produce a continuous flow, it takes 3 to 5 minutes, depending on the extrusion rate used. After continuous flow, the machine is run to perform specimen printing as in Fig. 6 a).

The resulting specimens were allowed to dry. At the time of drying, the size of the specimen will decrease due to shrinkage. It is one of the properties of PMMA and HA composites (Zebarjad et al, 2011). Some of the dried specimens are shown in Fig. 7. All specimens are then measured with a sliding range at the measurement points shown in Fig. 8. In addition, the printing time for each experiment is also recorded.

Figure 5. Continuous material flow

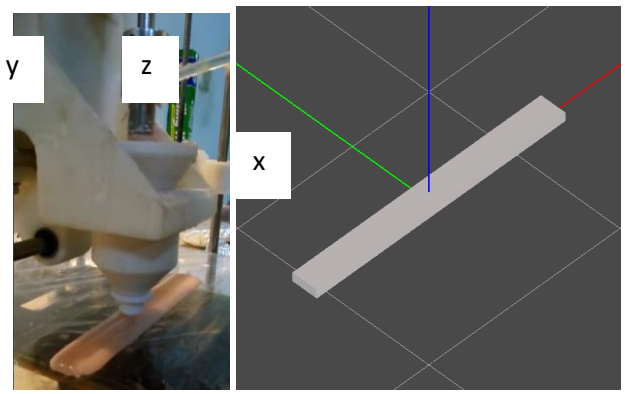

Figure 6. a) Printing process. b) Printing position

Figure 7. Specimen example

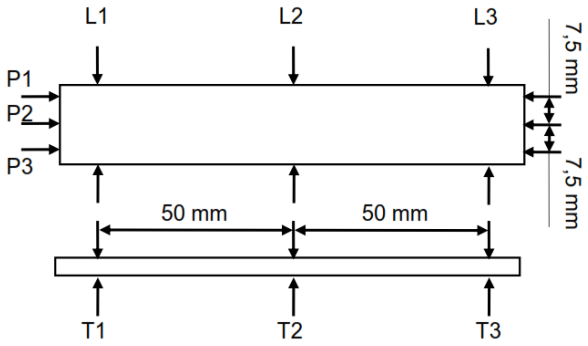

Figure 8. Specimen measurement points

RESULTS AND DISCUSSION

The specimen measurement results inserted into the Equ. (1), (2) and (3) to obtain an average of the measurement results as shown in Table 3.

$$\bar{P} = \frac{P1 + P2 + P3}{3} \quad (1)$$

$$\bar{L} = \frac{L1 + L2 + L3}{3} \quad (2)$$

$$\bar{T} = \frac{T1 + T2 + T3}{3} \quad (3)$$

Table 3. Printing time and average results of specimen measurement

RunOrder	Pbar (cm)	Lbar (cm)	Tbar (mm)	Waktu *Printing* (s)
1	13,10	2,26	4,67	221
2	12,89	1,84	3,82	274
3	13,10	2,14	3,73	216
4	13,06	2,39	3,70	283
5	13,05	2,46	3,33	296
6	12,91	1,92	3,62	216
7	13,12	2,22	3,53	173
8	13,43	2,56	3,33	186
9	13,32	2,64	3,10	182
10	12,68	2,15	3,27	201
11	13,14	2,56	3,93	293
12	12,81	2,46	4,03	182
13	13,29	2,24	4,00	211
14	12,64	2,15	3,43	396
15	13,20	2,43	3,40	170
16	13,18	2,62	3,27	211
17	12,53	1,99	4,03	216
18	12,62	2,35	3,87	215
19	12,69	2,32	4,13	213
20	12,84	2,30	4,02	216

Table 4 shows the results of descriptive statistical calculations for the overall responses. The result of descriptive statistical calculation shows that the average data of the measurement result of the specimen dimension is uniform. Pbar, or the average length is between 12.2 cm to 13.76 cm. Lbar or average width is between 1.62 cm to 2.98 cm. Tbar or average height is between 2.55 and 4.87 mm. However, on the printing time data, there is a longer printing time than the other printing time, i.e. in the 14th run.

Table 4. Printing time and descriptive statistics of average specimen measurement results

	Pbar	Lbar	Tbar	Printing time (s)
Mean	12,98	2,3	3,71	228,55
Median	13,055	2,31	3,72	215,5
Modus	13,1	2,46	3,33	216
Skewness	-0,16	-0,38	0,53	1,72
Kurtosis	-1,01	-0,43	0,33	3,48
Standard Deviation	0,26	0,23	0,39	54,73
LCL	12,20	1,62	2,55	64,35
UCL	13,76	2,98	4,87	392,75

The average specimen measurement result is then inserted into Equ. (4) to get data errors as shown in Fig. 9, Fig. 10 and Fig. 11. Dimension errors shows the dimensional difference percentage of specimens that have been so with the dimensions of the specimen on the design. The percentage of dimensional error is shown with graphs in Fig. 9, 10, and 11.

$$\text{Dimensional errors (\%)} = \left| \left[\frac{\text{part dimension-design dimension}}{\text{design dimension}} \right] \times 100\% \right| \quad (4)$$

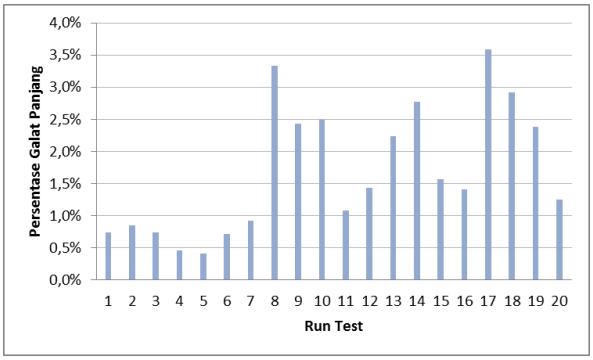

Figure 9. Percentage of length errors for each run test

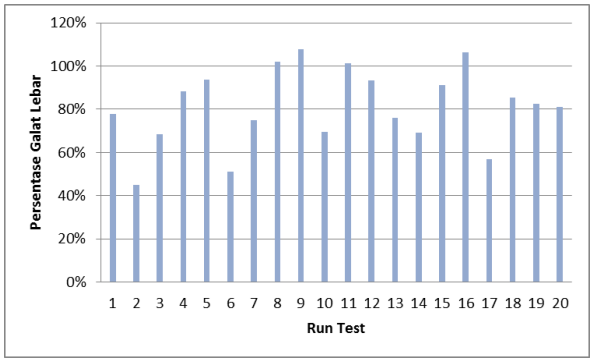

Figure 10. Percentage of width error for each run test

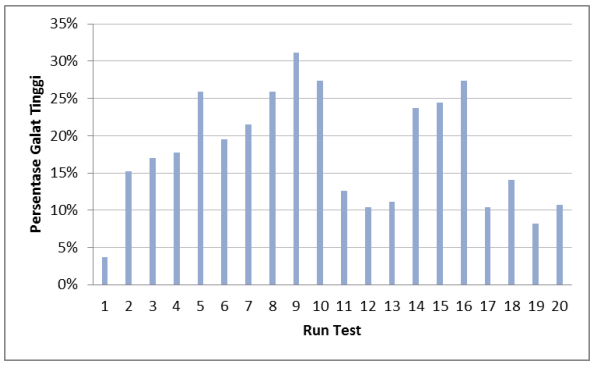

Figure 11. Percentage of thickness errors for each run test

Of all the run tests, the highest percentage error rate was found in the seventh run test, which was 3.6%. The lowest percentage of length error was found in the fifth run test, which is 0.4%. Compared to width errors and thickness errors, the resulting length error is the lowest error. However, an error value below 0.5% is only generated in the fifth run test.

Width error values are the highest error among other error values. Most of the width error values are above 50%. The smallest width error is 44.9%, while the largest width error is 107.9%, meaning the width of some specimens generated reaches more than twice the size of the design width. At the time the specimen is printed, dried to shrank, the size of the specimen width is larger than the design.

Most of the thickness error values are not as wide as the error value, but the overall value is above 0.5%. The smallest value of the thick error is 3.7%, while the largest value of the thick error is 31.1%.

Dimensional errors may occur due to shrinkage of specimens as described earlier. In addition, dimensional error may also be affected by printing orientation (Wang et al, 2007; Tanoto et al, 2017). Each printing orientation will produce different dimension errors for each side of the print output. In this study, the position of specimen printing is arranged as in Fig. 6 b) in order that the bottom is the widest side. Machines work on long sides or x-axis (130 mm) in longer time than work on the width or y-sides (12.7 mm). As a result, more pastes were deposited when printing long sides. This causes the width error to be generated larger than other dimensional errors.

The overall error data obtained is then analyzed by Minitab 17 software. The goal is to know the effect of each or the interaction of two or three parameters used against dimensional error. The result of calculation with analysis of variance (ANOVA) is shown in Table 4.

Table 4. ANOVA test resullt

		Length error		Width error		Thickness error	
	DF	**F_{value}**	**P_{value}**	**F_{value}**	**P_{value}**	**F_{value}**	**P_{value}**
Model	10	0,78	0,649	0,53	0,832	0,74	0,679
Blok	1	3,98	0,077	0	1,0	0,53	0,486
Linear	3	0,6	0,634	0,65	0,604	0,17	0,914
PS	1	0,76	0,407	1,34	0,276	0,38	0,555
IS	1	0,59	0,462	0,23	0,641	0,1	0,755
FA	1	0,44	0,524	0,36	0,561	0,03	0,869
Square	3	0,17	0,913	0,66	0,595	1,16	0,378
PS*PS	1	0	0,999	0,67	0,433	2,44	0,153
IS*IS	1	0,2	0,668	0,87	0,375	0,69	0,426
FA*FA	1	0,28	0,61	0,73	0,415	0,1	0,758
Inter-Aksi 2 Jalur	3	0,51	0,685	0,45	0,721	0,96	0,453
PS*IS	1	0,32	0,586	1,2	0,302	1,32	0,28
PS*FA	1	0,05	0,829	0,04	0,85	0,86	0,377
IS*FA	1	1,16	0,309	0,13	0,728	0,7	0,426
Error	9	-	-	-	-	-	-
Lack of Fit	5	0,93	0,544	1,09	0,479	0,34	0,865
Pure Error	4	-	-	-	-	-	-
Total	19						

When compared with Ftable or F0,05; 5; 4 = 6,26, Fvalue value for the third dimension error is smaller, both from the influence of each variable and the interaction between variables. When compared with α = 0.05, the Pvalue value for all three dimensional errors is greater. This shows that there is no significant difference between the prints in one run test and the prints in the other test runs. By setting machine parameters within the range of values in Table 1, the 3D printing machine prints in almost the same time range for all specimens. Therefore, the size of the resulting specimen is almost the same. Nevertheless, the resulting error is still relatively high. Therefore, it is necessary to evaluate other machine parameters or other parameters that may affect dimensional error.

When compared to Ftable or F0,05; 5; 4 = 6.26, the Fvalue for the third dimension error is smaller, both seen from the influence of each variable and the interaction between variables.

When compared with α = 0.05, the Pvalue for all three dimensional errors is greater. This shows no significant difference between the printing result in one run test and printing result in the other test runs. By setting the machine parameters within the value range in Table 1, the 3D printing machine prints in almost the same time range for all specimens. Therefore, the size of the resulting specimen is almost the same. However, the percentage error is still high. Therefore, it is necessary to evaluate other machine parameters or other parameters that may affect dimensional error.

CONCLUSION

The parameters of machine settings tested in this study, i.e. perimeter speed, infill speed, and fill angle, have no significant effect on specimen dimension. The machine can print specimen in simple shape with almost the same dimensions for each printing run with the parameters settings that have been tested. There may be other parameters that may affect dimensional differences. The resulting product dimension error is still high. Therefore, in further research, there should be assessment to determine other factors that affect dimension error. For example by adjusting dimensions on product design or modification of nozzle size on 3D printing machine. By identifying these factors, it is expected to print products with smaller dimensional errors.

Nomenclature

Pbar = Average Length
Lbar = Average Width
Tbar = Average Thickness
PS = Perimeter Speed
IS = Infill Speed
FA = Fill Angle

ACKNOWLEDGEMENT

We would like to express our gratitude to PUPT, Directorate of Research and Community Service, Directorate General of Research and Development, Ministry of Research, Technology and Higher Education in accordance with the Contract of Research of fiscal year 2017 with contract number: 001 / SP2H / LT / DRPM / IV / 2017.

REFERENCES

Bezerra, M.A., Santelli, R.E., Oliveira, E.P., Villar, L.S. and Escaleira, L.A. (2008). Response Surface Methodology (RSM) as a Tool for Optimization in Analytical Chemistry. *Talanta.* 76(5): 965-977. http://dx.doi.org/10.1016/j.talanta.05.019

Castelan, J., Schaeffer, L., Daleffe, A., Fritzen, D., Salvaro, V., and Silva, F. P. (2014). Manufacture of Custom-made Cranial Implants from DICOM® Images Using 3D *Printing*, CAD/CAM Technology and Incremental Sheet Forming. *Revista Brasileira de Engenharia Biomédica*. 30(3): 265-73. http://dx.doi.org/10.1590/rbeb.2014.024

Köksal, G., Batmaz, İ., and Testik M.C. (2011). A Review of Data Mining Applications for Quality Improvement in Manufacturing Industry. *Expert Systems with Applications*. 38(10): 13448-67. http://dx.doi.org/10.1016/j.eswa.2011.04.063

Lamboni, L., Gauthier, M., Yang, G., Wang, Q. (2015). Silk Sericin: A Versatile Material for Tissue Engineering and Drug Delivery. *Biotechnology Advances*. 33(8): 1855-1867. http://dx.doi.org/10.1016/j.biotechadv.2015.10.014

Lim, G., Choi, D. and Richardson, E.B. (2014). 3-D Printing in Organ Transplantation. *Hanyang Medical Reviews*. 34(4): 158-164. http://dx.doi.org/10.7599/hmr.2014.34.4.158

Mohammed, M., Fitzpatrick, A., Malyala, S., and Gibson, I. (2016). Customised Design and Development of Patient Specific 3D Printed Whole Mandible Implant. *Proceedings of the 27th Annual International Solid Freeform Fabrication Symposium.* Texas, US. 1708-1717.

Mohamed, O.A., Masood, S.H. and Bhowmik, J.L. (2015). Optimization of Fused Deposition Modeling Process Parameters: a Review of Current Research and Future Prospects. *Advances in Manufacturing*. 3(1): 42-53. http://dx.doi.org/10.1007/s40436-014-0097-7

Tanoto, Y.Y., Anggono, J., Siahaan, I.H., and Budiman, W. (2017). The Effect of Orientation Difference in Fused Deposition Modeling of ABS Polymer on The Processing Time, Dimension Accuracy, and Strength. *AIP Conference Proceeding*, 1788(1). http://dx.doi.org/10.1063/1.4968304

Tontowi, A.E., Anggraeni, D., Saragih, H.T., Raharjo, K.P.N., and Utami, P. (2017). Experimental Study of 3D-printable Biocomposite of [HA/PMMA/Sericin] Materials. *Advanced Materials Letters*. 2017; 8(8): 857-861.

Puska, M., Aho, A.J. and Vallittu, P. (2011). Polymer Composites for Bone Reconstruction. *INTECH Open Access Publisher*. http://dx.doi.org/10.5772/20657

Schickert, S.D.L. (2014). Polymer-ceramic Nanocomposites for Bone Regeneration. *Doctoral dissertation*. Instituto de Ciencias da Saude.

Serbetci, K., Korkusuz, F. and Hasirci, N. (2004). Thermal and Mechanical Properties of Hydroxyapatite Impregnated Acrylic Bone Cements. *Polymer Testing*. 23(2): 145-155. http://dx.doi.org/10.1016/S0142-9418(03)00073-4

Wang, C.C., Lin, T.W., Hu, S.S. (2007). Optimizing the Rapid Prototyping Process by Integrating the Taguchi Method with the Gray Relational Analysis. *Rapid Prototyping Journal*. 13(5): 304-315. http://dx.doi.org/10.1108/13552540710824814

Wang, X., Jiang, M., Zhou, Z., Gou, J. and Hui, D. (2016). 3D *Printing* of Polymer Matrix Composites: A Review and Prospective. *Composites Part B: Engineering*. 110: 442-458. http://dx.doi.org/10.1016/j.compositesb.2016.11.034

Zebarjad, S.M., Sajjadi, S.A., Sdrabadi, T.E., Yaghmaei, A., and Naderi, B. (2011). A Study on Mechanical Properties of PMMA/ Hydroxyapatite Nanocomposite. *Engineering*. 3(8): 795-801. http://dx.doi.org/10.4236/eng.2011.38096